1

Wearable Organic Nano-sensors

Wei Huang[1], Liangwen Feng[2], Gang Wang[3,4], and Elsa Reichmanis[4]

[1] University of Electronic Science and Technology of China (UESTC), School of Optoelectronic Science and Technology, No. 4, Sec. 2, North Jianshe Rd, Chengdu 610054, China
[2] Chinese Academy of Sciences, The State Key Laboratory of Organometallic Chemistry, Shanghai Institute of Organic Chemistry, 345 Lingling Lu, Shanghai 200032, China
[3] Donghua University, State Key Laboratory for Modification of Chemical Fibers and Polymer Materials, College of Material Science and Engineering, 2999 North Renmin Road, Shanghai 201620, People's Republic of China
[4] Georgia Institute of Technology, School of Chemical and Biomolecular Engineering, School of Chemistry and Biochemistry, and School of Materials Science and Engineering, Atlanta, GA 30332, USA

1.1 Introduction

The development of unconventional electronics, or the Internet of Things (IoT), which enables active connections between various electronic devices and massive information flows from both the environment and humans, will likely lead to another technology revolution in the near future [1]. To realize effective connections between factors such as environmental parameters and human vital statistics and electronic devices, sensors serving as an inevitable bridge that converts environmental/human body signals to electronic signals and their characteristics will determine the future of IoT [2].

Nowadays, numerous sensors, including optical, chemical, electrical, gas, heat, and mechanical, already play an important role in our daily life [3]. For instance, a typical smartphone contains an accelerometer, gyroscope, magnetometer, proximity sensor, ambient light sensor, microphone, touchscreen sensor, etc. These sensors enable us to live better, learn quicker, and work faster [4]. Even though enormous achievements have been realized with these state-of-the-art sensors, they continue to provide us with emerging applications, including humidity sensors that can be integrated into a cellphone and optical sensors that are able to recognize a human face. These successfully commercialized sensors rely on traditional inorganic mechanically rigid materials and complex fabrication processes, which are usually not compatible with flexible/stretchable substrates [5].

In recent decades, another kind of electronic material consisting of organic components has emerged as an attractive alternative [6]. Compared to its inorganic counterparts, organic materials, in theory, possess unlimited species, since the properties of organic materials can be manipulated by simply regulating the chemical structures and/or compositions [7]. Organic semiconductors (OSCs)

Flexible and Wearable Electronics for Smart Clothing, First Edition.
Edited by Gang Wang, Chengyi Hou, and Hongzhi Wang.

have already accelerated the development of flat panel displays due to the incredibly high performance of organic light-emitting diodes (OLEDs). Organic thin-film transistor (OTFT) based back panel displays also give rise to the commercialization of the first ever bendable smartphone [8]. A plastic empire is on the rise, as a large fraction of the organic materials are polymers, and they are utilized in almost every aspect of daily life in the human society [8]. Polymers can be designed to be stronger than metals, as reliable as ceramics, and as soft as liquids. More interestingly, they can be constructed to be insulators, semiconductors, or even conductors. Unconventional properties, such as self-healing, and stretchable semiconductors/conductors can also be accomplished with organic materials [9].

Taking advantage of the wide range of properties of organic materials, multifunctional sensors with flexibility/stretchability are rapidly developing and as a result, the design of wearable sensors has become a major research target. The next-generation sensors should be low-cost, lightweight, low energy consuming devices, which together with capabilities such as being bendable or even stretchable, will ensure compatibility with wearable technologies. Wearable sensors can not only simplify the daily life routine but also provide a great tool for in situ monitoring of either external or internal parameters [10]. People have already partially benefited from wearable sensors; applications to monitor heart rate (or even electrocardiography) and the number of steps walked are already commonplace in smart watches. In the future, wearable sensors will enable real-time monitoring of the health of the human body, including blood pressure, oxygen levels or if someone has suddenly fallen, and will likely enable quick diagnosis of common diseases [11]. Furthermore, environmental conditions and hazardous atmospheric conditions can be monitored, which can act as information collection terminals in IoT, improving public safety [12].

1.2 Wearable Organic Sensors Based on Different Device Architectures

Owing to the boost in the area of organic electronic materials, different device architectures can be adopted to realize flexible and stretchable organic sensors for potentially wearable applications. Among various device architectures, resistors, transistors, electrochemical, and diode-based devices are intensively investigated, owing to their compatibility with traditional Si processing. While different device architectures have different advantages, they can all be designed to function as effective sensors. Sensing applications, including motion detection, hazardous gas monitoring, disease diagnosis, temperature recording, etc. will be summarized. Furthermore, the integration of wearable sensors with portable power sources and data processing hardware/software to enable real-time information collection and processing has been reported [13].

In the following sections, we will focus on different sensor device structures, illuminating the functional principles, popular organic materials, and practical applications. Representative examples for designing flexible/stretchable sensors and the strategies to enhance the sensing performance will be demonstrated.

1.2.1 Resistor-Based Sensors

1.2.1.1 Definitions and Important Parameters

One of the simplest electronic devices is the resistor, where resistance is the key parameter for any type of resistor. By utilizing resistors as sensors, the variation in resistance is recorded when the resistor is in contact with the analyte. Not only the value of the resistance is important for sensor applications, but several other parameters are also equally critical. These include response time and recovery time, which indicate how long the sensor will generate effective processable signals or recover to its original state, and sensitivity, which indicates the detection limit of a target analyte. As resistors are easily fabricated and characterized, they represent the most widely studied device structure for sensing applications, including sensors with stretchable and wearable properties.

1.2.1.2 Materials and Applications

Materials are the most important factor influencing sensor performance, contributing to the direct interaction with the analyte and electronic signal transformation. Among all the materials that can be used as active layers in a resistor-based sensor, graphene has exhibited emerging advantages due to its high surface to volume ratio, controllable conductivity by adjusting the composition/morphology/geometry, and excellent thermal conductivity. Wang and coworkers successfully demonstrated a highly conductive, flexible, and compressible all-graphene thin-film sensor [14]. This sensor can sense heat and cold, measure the dimensions of the heated/cooled area, discern human touch from other pressures, and enable human touch location and measurement of pressure level under zero working voltage. Graphene was also coupled with some organic materials to improve the sensing performance. The passive all-graphene flexible thin-film sensor (FTS) technology may pave new pathways for the development of electronic skin.

In another example, Zhu and coworkers fabricated highly sensitive graphene woven fabrics (GWFs) by using a crisscross copper mesh substrate with chemical vapor deposition (CVD) of graphene [15]. A flexible and wearable strain sensor was assembled by adhering the GWFs on polydimethylsiloxane (PDMS) and medical composite tape. The ultralight sensor exhibited features including relatively good sensitivity, high reversibility, superior physical robustness, easy fabrication, ease to follow human skin deformation without irritation, and so on. As a consequence of the piezoresistive effect of GWFs, the sensors were used as electronic skin covering the human body to detect body motions (Figure 1.1a,b). The signals of GWF resistance change depend on the deformation strain that is formed by the motions. The stronger the motion, the larger the strain, and the motion signals can be recorded more easily. Some weak human motions were chosen to test the notable resistance change, including hand clenching, phonation, expression change, blink, breath, and pulse. Because of the distinctive features of high sensitivity and recyclability, the GWFs–PDMS–tape based piezoresistive sensors exhibited wide potential applications in displays, robotics, fatigue detection, body monitoring, in vitro diagnostics, and advanced therapies.

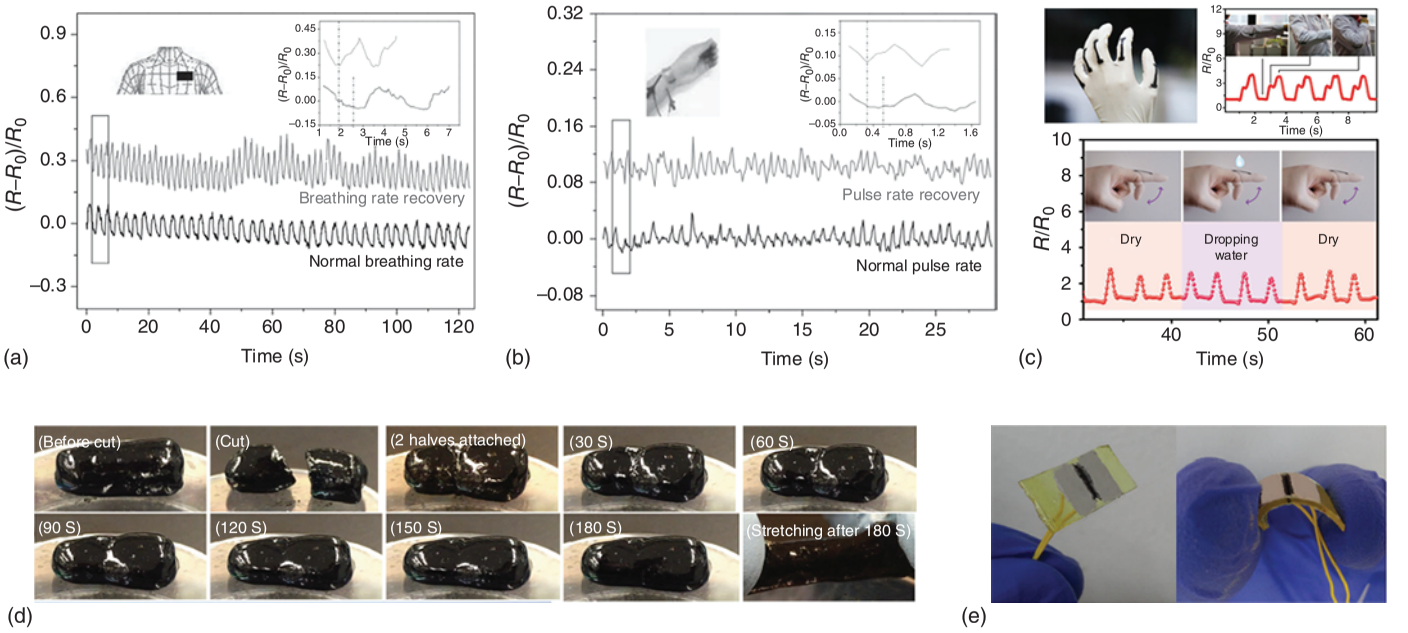

Figure 1.1 Relative change in resistance of respiration and pulse, in (a) and (b), respectively, at still state and exercise state. (c) Real-time human motion detection using superhydrophobic MWCNT/TPE-film sensors, including an optical photograph of a latex glove with five film sensors coated on each finger; normalized relative resistance as a function of time; and real-time variation of the normalized relative resistance. (d) Self-healing property of H2010h1 hydrogel. The hydrogel was cut into two halves and then brought together again; every 30 seconds, the hydrogel is shown enabling us to track the vestige of cut. (e) Photograph of the self-healing chemiresistor consisting of a transparent (yellowish) self-healing substrate, jelly-like self-healing electrode, and pliable induced self-healing AuNP film. Source: (a, b) Wang et al. 2014 [15]. Reproduced with permission of John Wiley & Sons; (c) Li et al. 2017 [19]. Reproduced with permission of John Wiley & Sons; (d) Darabi et al. 2017 [20]. Reproduced with permission of John Wiley & Sons; (e) Huynh and Haick 2016 [21]. Reproduced with permission of John Wiley & Sons.

Further, Lee and coworkers reported a flexible and transparent chemical sensor comprising reduced graphene oxide (rGO) coupled with organic dye molecules (bromophenol blue) [16]. This device possesses promising properties such as high mechanical flexibility (>5000 bending cycles with a bending radius of 0.95 cm) and optical transparency (>60% in the visible region). Stacking the water-trapping dye layer on rGO enabled a higher response in a large relative humidity range (up to 80%), and dual-mode detection capabilities of colorimetric and electrical sensing for NH_3 gas (5–40 ppm). These advantages were attributed to the flexible and transparent rGO sensor coupled with organic dye molecules, providing great potential for real-time monitoring of toxic gas/vapor in future practical chemical sensing at room condition in wearable electronics.

Carbon nanotubes (CNTs) are another attractive material [17]. As one of the most promising semiconducting materials that may replace traditional Si, CNTs, which can act as core active materials in next-generation electronics, have also been adopted in sensing. Karimov et al. designed a CNT-based Al/CNT/Al pressure sensor [18]. This sensor was fabricated by depositing CNTs on an adhesive elastic polymer tape and placing it into an elastic casing. The diameter of multiwalled nanotubes varied between 10 and 30 nm. The nominal thickness of the CNT layers in the sensors was in the range ~300–430 μm. The interelectrode distance (length) and the width of the surface-type sensors were in the ranges 4–6 and 3–4 mm, respectively. The resistance of the sensors decreased by three to fourfold as the pressure was increased up to 17 kN/m^2. Similar to graphene, researchers also mixed CNTs with other materials to enable enhanced performance. Zhang and coworkers fabricated a highly flexible multifunctional smart coating by spray-coating multiwalled CNTs dispersed in a thermoplastic elastomer solution, followed by treatment with ethanol [19]. The coatings not only endowed various substrate materials with superhydrophobic surfaces but also responded to stretching, bending, and torsion – properties useful for flexible sensor applications (Figure 1.1c). The coatings exhibited superior sensitivity (gauge factor of 5.4–80), high resolution (1° of bending), fast response time (<8 ms), stable response over 5000 stretching–relaxing cycles, and wide sensing ranges (stretching: over 76%, bending: 0°–140°, torsion: 0–350 rad/m). Moreover, multifunctional coatings with thicknesses of only 1 μm can be directly applied to clothing for full-range and real-time detection of human motions. These sensors also showed extreme repellency to water, acid, and alkali, improving the work stability under wet and corrosive conditions.

Polymers are another widely used material for resistor-based sensing, since most polymers are intrinsically flexible/stretchable and can be engineered to be either insulators or (semi)conductors. Most of the research concerning polymer sensors is realized by utilizing/incorporating active polymer materials. In recent years, self-healing polymers represent a highlight in wearable sensors, since the self-healing characteristics provide durability upon bending and stretching. Among all potential candidates, hydrogels with excellent biocompatibility and mechanical features close to human tissues constitute a promising avenue for realizing health-care-oriented electronic functionalities. Xing and coworkers reported the development of a mechanically and electrically self-healing hydrogel based on physically and chemically cross-linked networks (Figure 1.1d) [20].

Autonomous intrinsic self-healing of the hydrogel was attained through dynamic ionic interactions between carboxylic groups of poly(acrylic acid) and ferric ions. Covalent cross-linking was used to support the mechanical structure of the hydrogel. Establishing a fair balance between the chemical and physical cross-linking networks together with the conductive nanostructure of polypyrrole networks led to a double network hydrogel with bulk conductivity, mechanical and electrical self-healing properties (100% mechanical recovery in two minutes), ultrastretchability (1500%), and pressure sensitivity. The practical potential of hydrogels is further revealed by their application in human motion detection and their 3D-printing performance. Mixing self-healing polymers with other active materials was also adopted in sensors. Huynh and Haick synthesized a self-healing polymer and composite (with Au nanoparticles, AuNPs) and assembled a bendable and stretchable self-healing chemiresistor for pressure/strain, temperature, and volatile organic compounds (VOCs) sensing (Figure 1.1e) [21]. Pressure/strain and temperature sensitivity was highly comparable to available flexible sensors. The limit of detection for VOCs in the parts per billion range makes the device useful for sensing VOCs. Healing efficiency of this chemiresistor is high so that the sensor survived after cutting several times at random positions. Moreover, the sensor was environmentally stable, i.e. the sensitivity slightly decreased (<10%) after six months. Three different chemiresistive AuNPs were used for this chemical sensor, proving its versatile combination of self-healing polymers with different sensing materials. The reported self-healing sensor raises expectations that flexible devices might one day become self-administered, thus increasing their reliability in various applications, such as durable-transparent touch-screens, self-healing e-skins, and implantable health-care electronics.

On the other hand, biocompatible polymers are also of interest for wearable sensors. To date, most reported skin-like pressure sensors are based on nanomaterials and microstructured PDMS films, limiting their wide practical applications due to unknown biotoxicity and the redundant fabrication procedure. A cost-effective, large-area-capable, and biocompatible approach for fabrication of high-performance skin-like pressure sensors is highly desired. Silk fibroin (SF) is a natural protein that has recently drawn attention due to its application as a substrate for flexible electronics.

As shown in Figure 1.2, Zhang and coworkers demonstrated the fabrication of skin-like pressure sensors using SF-derived active materials [22]. Flexible and conformal pressure sensors were fabricated using transparent carbonized silk nanofiber membranes (CSilkNM) and unstructured PDMS films through a cost-effective and large-scale capable approach (Figure 1.2a–e). Owing to the N-doped carbon nanofiber network structure of CSilkNM, the obtained pressure sensor shows superior performance, including ultrahigh sensitivity ($34.47\,kPa^{-1}$) for a broad pressure range, an ultralow detection limit (0.8 Pa), rapid response time (<16.7 ms), and high durability (>10 000 cycles). Based on its superior performance, the applications in monitoring human physiological signals, sensing subtle touch, and detecting spatial distribution of pressure were also demonstrated. Not only can the chemical structure be modified to realize high-performance sensors, but the dimensional structural design can also lead

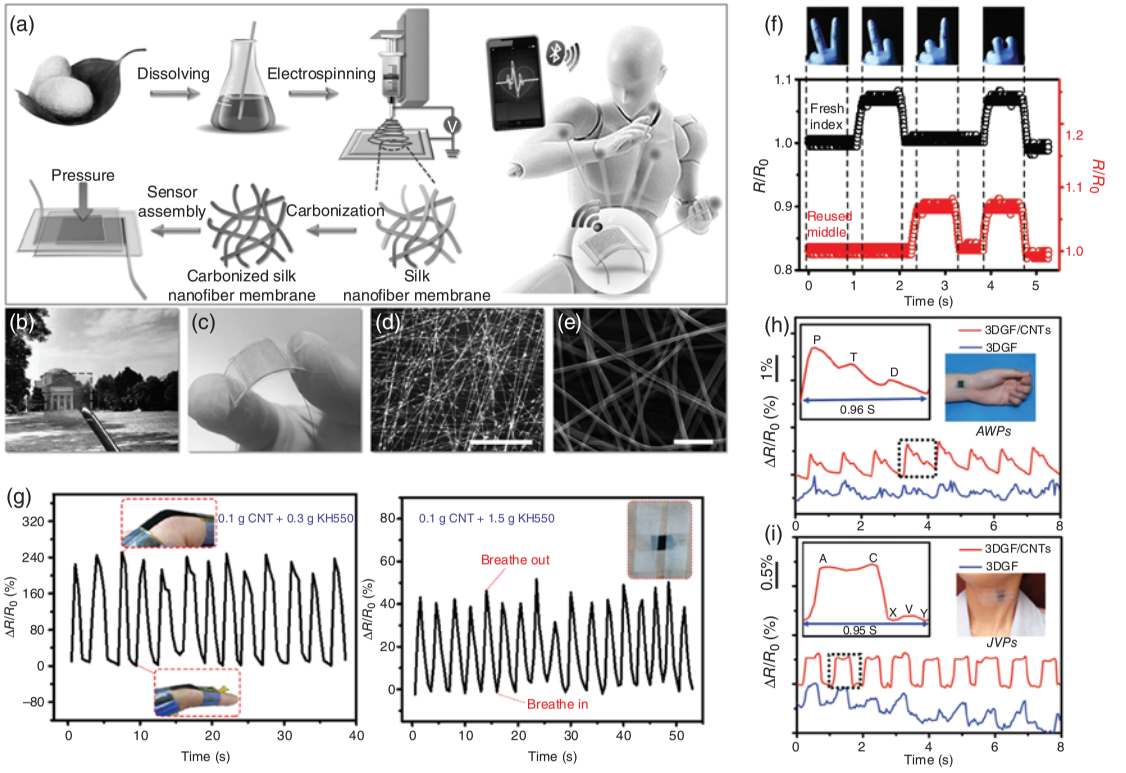

Figure 1.2 Fabrication process and structure of the CSilkNM pressure sensor. (a) Schematic illustration showing the fabrication process of CSilkNM pressure sensors. Photographs showing the (b) transparency and (c) flexibility of the obtained sensor. (d) Optical image of a silk nanofiber membrane. Scale bar: 100 μm. (e) SEM image of CSilkNM. Scale bar: 1 μm.(f) The dual sensing result from a fresh hydrogel sensor (index finger, black) and a reusable (after 12 drying–soaking cycles) hydrogel sensor (middle finger, red) reveals that the as-fabricated hydrogel electronics is able to simultaneously detect motions of multiple objects without cross-impact. (g) The relative resistance change of the sensor (0.1 g CNT/0.3 g KH550) in hand motion from stretch to curve, and the relative resistance change of the sensor (0.1 g CNT/1.5 g KH550) in response to breathing. (h) Real-time and in situ AWP measurement with the 3DGF/CNT and 3DGF networked skin-attachable strain sensor attached on the wrist. The inset shows the photograph and zoomed waveform. (i) Measurement of JVPs with strain sensors attached on the neck. The inset is the photograph and zoomed waveform. Source: (a–e) Wang et al. 2017 [22]. Reproduced with permission of John Wiley & Sons; (f) Liu et al. 2018 [23]. Reproduced with permission of John Wiley & Sons; (g) Zhou et al. 2018 [25]. Reproduced with permission of American Chemical Society; (h, i) Cai et al. 2017 [26]. Reproduced with permission of John Wiley & Sons.

to superior performance. Xu and coworkers proposed a simple paradigm to prototype stretchable electronics with an embedded three-dimensional (3D) helical conductive layout based on biocompatible and stretchable hydrogels [23]. Thanks to the 3D helical structure, hydrogel electronics presents satisfactory mechanical and electrical robustness under stretch. In addition, reusability of stretchable electronics is realized with the proposed scenario benefiting from the swelling property of hydrogel. Although losing water would induce structural shrinkage of the hydrogel network and further undermine the function of the hydrogel in various applications, the worn-out hydrogel electronics can be reused by simply casting it in water. Through such a rehydration procedure, the dehydrated hydrogel can absorb water from the surroundings and then the hydrogel electronics can achieve resilience in mechanical stretchability and electronic functionality. Also, the ability to reflect pressure and strain changes has revealed hydrogel electronics to be promising for advanced wearable sensing applications (Figure 1.2f).

One classical way using multiple active materials within a single device is widely adopted in resistor-based sensors. A mixture of graphene and stretchable polymers was investigated by Ren and coworkers, who demonstrated a mechanical sensor fabricated using a graphene porous network (GPN) combined with PDMS [24]. Using nickel foam as a template and a chemical etching method, the GPN can be created in the PDMS-nickel foam coated with graphene. The resultant material achieved both pressure and strain sensing properties. Because of the pores in the GPN, the composite sensor exhibited a wide pressure sensing range and highest sensitivity among graphene foam-based sensors. In addition, it showed potential for use in applications such as monitoring or even recognizing walking states, the degree of finger bending, and wrist blood pressure. Fu and coworkers reported a new method to realize control on the local conductive networks of strain sensors, and thus their sensing behavior [25]. They spray-coated a mixture of CNTs and 3-aminopropyltriethoxysilane (KH550) with various ratios onto PDMS to prepare multifunctional crack-based sensors. The conductive CNT/KH550 layer exhibited brittle mechanical behavior, which triggered the formation of cracks upon stretching. This is thought to be responsible for the observed electromechanical behavior. These sensors exhibited adjustable gauge factors of 5–1000, stretchability (ε) of 2–250%, linearity (nonlinearity–linearity), and high durability over 1000 stretching–releasing cycles for mechanical deformation. Washable, wearable, and water-repellent sensors were prepared through such a method to successfully detect human physiological activities (Figure 1.2g). Moreover, the variation in temperature or the presence of solvent could also be detected due to the thermal expansion and swelling of the PDMS layer. It is expected that such a concept could be used to fabricate sensors for multiple applications, thanks to its multifunctionality, adjustable and robust performance, and simple and low-cost fabrication strategy.

Separately, Dong and coworkers demonstrated epidermal sensors based on an all-carbon collaborative percolation network, which consists of 3D graphene foam and CNTs obtained by two-step CVD processes [26]. The nanoscaled CNT networks largely enhance the stretchability and signal-to-noise ratio (SNR) of the 3D microarchitectural graphene foams, endowing the strain sensor with a

gauge factor as high as 35, a wide reliable sensing range up to 85%, and excellent cycling stability (>5000 cycles). The flexible and reversible strain sensor can be easily mounted on human skin as a wearable electronic device for real-time and high-accuracy detection of electrophysiological stimuli and even for acoustic vibration recognition (Figure 1.2h,i). The rationally designed all-carbon nanoarchitectures are scalable, low cost, and promising in practical applications requiring extraordinary stretchability and ultrahigh SNRs. Lubineau and coworkers proposed transformation of an electrically conductive material from a sensor to a conductor using electrical welding (e-welding) [27]. This method is demonstrated in the case of a thermoplastic polymer sponge decorated with silver nanowires. The sensor-like behavior of the sponge was programmed by e-welding into conductor-like behavior, i.e. suppressing the gauge factor by 86%, without varying the density of the silver nanowires. An application of e-welding in the fabrication of a sensor-conductor hybrid material that may be applied as soft artificial skin in robotics was demonstrated.

1.2.2 Organic Field-Effect Transistor Based Sensors

1.2.2.1 Definitions and Important Parameters

The transistor, the base of modern electronics, is usually configured as a three-terminal device (including a gate electrode, and source and drain electrodes), where the gate electrode accompanied with a dielectric can effectively modify the carrier concentration of the semiconductor, leading to controllable drain current. Key parameters associated with transistor operation are mobility, threshold voltage, on/off ratio, and subthreshold swing. However, in a transistor-based sensor, the sensitivities and the response/recovery time are the dominant parameters for practical applications [28]. Compared with resistors, even though transistor-based sensors are more complicated in device structure, they have the advantage of multiparameter sensing capabilities [29]. All the key parameters, which include but are not limited to mobility, threshold voltage, turn-on voltage, off-current, and on-current, can be used to detect the influence of analytes on the device [30]. Moreover, since transistors can be operated under various gate biases and may be designed to amplify the current, such sensors have the potential to realize ultrahigh sensitivity [31]. Furthermore, since the active components in a transistor are richer than in a resistor, one can enhance the sensing performance by not only changing the semiconducting materials, but also the dielectric and electrode materials.

1.2.2.2 Strategy and Applications

Transistors based on OSCs are widely explored in the area of sensing [32]. Modifying the organic semiconducting layer is the most common way to improve transistor sensing parameters, where strategies including using thinner OSC films, organic nanowires, coupling with other analyte receptors are generally used. Perhaps the most common way to optimize sensor performance is to utilize an OSC that is intrinsically sensitive. As shown in Figure 1.3a, Noh and coworkers reported a highly sensitive printed ammonia (NH_3) gas sensor based on OTFTs fabricated with the fluorinated difluorobenzothiadiazole-dithienosilole

polymer (PDFDT) [33]. The sensor detected NH_3 down to 1 ppm with high sensitivity using bar-coated ultrathin (<4 nm) PDFDT layers in the absence of any receptor additives (Figure 1.3b,c). The sensing mechanism was confirmed by cyclic voltammetry, hydrogen/fluorine nuclear magnetic resonance, and UV/visible absorption spectroscopy. PDFDT–NH_3 interactions comprise hydrogen bonds and electrostatic interactions between the PDFDT polymer backbone and NH_3 gas molecules, thus lowering the highest occupied molecular orbital levels, leading to hole trapping in the OTFT active layer. Additionally, density functional theory calculations demonstrated that gaseous NH_3 molecules were captured via cooperation of fluorine atoms and dithienosilole units in PDFDT. They verified that incorporation of functional groups that interact with a specific gas molecule in a conjugated polymer presents a promising strategy for producing high-performance printed OTFT gas sensors. Sensitive organic semiconducting materials were also applied in photo-sensors.

Qiu and coworkers prepared flexible and low-voltage near-infrared organic phototransistors (NIR OPTs) with a low-bandgap donor–acceptor conjugated polymer as the semiconductor layer and *n*-octadecyl phosphonic acid modified anodic alumina (AlO_x/ODPA) as the insulating layer (Figure 1.3d) [34]. The phototransistors exhibited typical n-channel transistor characteristics at a voltage below 5 V. The photosensitivity can be enhanced by regulating the packing densities of the ODPA self-assembled monolayers and forming different trap states. The enhanced organic phototransistors (OPTs) exhibited good photosensitivity to 808–980 nm near-infrared (NIR) with the photocurrent/dark current ratio and photoresponsivity as high as 5×10^3 and 20 mA/W, respectively, benefiting from the charge-trapping effect at the AlO_x/ODPA interface, as shown in Figure 1.3e. The OPTs also presented a fast-optical switching speed of 20/30 ms and excellent mechanical flexibility. The outstanding performance of the NIR OPTs indicates that the development of wearable electronics is, indeed, possible.

Research on dielectrics has also been applied to the development of transistor-based sensors as a means to enhance performance. Huang and coworkers demonstrated a highly thermally stable organic transistor by applying a three-arm stereocomplex polylactide (tascPLA) as the dielectric and substrate material [35]. The resulting flexible transistors were stable up to 200 °C, while devices based on traditional polylactide (PLA) were damaged at 100 °C. Furthermore, the charge-trapping effect induced by polar groups of the dielectric was also utilized to significantly enhance the temperature sensitivity of the electronic devices. A skin-like temperature sensor array was successfully demonstrated based on such transistors, which also exhibited good biocompatibility in cytotoxicity measurements. By presenting the combined advantages of transparency, flexibility, thermal stability, temperature sensitivity, degradability, and biocompatibility, these organic transistors possess broad applicability in applications such as environmentally friendly electronics, implantable medical devices, and artificial skin. Good dielectric performance can enhance the sensitivity and lower the driving voltage at the same time. Zheng and coworkers developed controllable polyelectrolyte composites based on poly(ethylene glycol) (PEG) and polyacrylic acid (PAA) as a type of high capacitance dielectric for flexible OTFTs and ultrasensitive pressure sensors with sub-1 V operation (Figure 1.3f) [36].

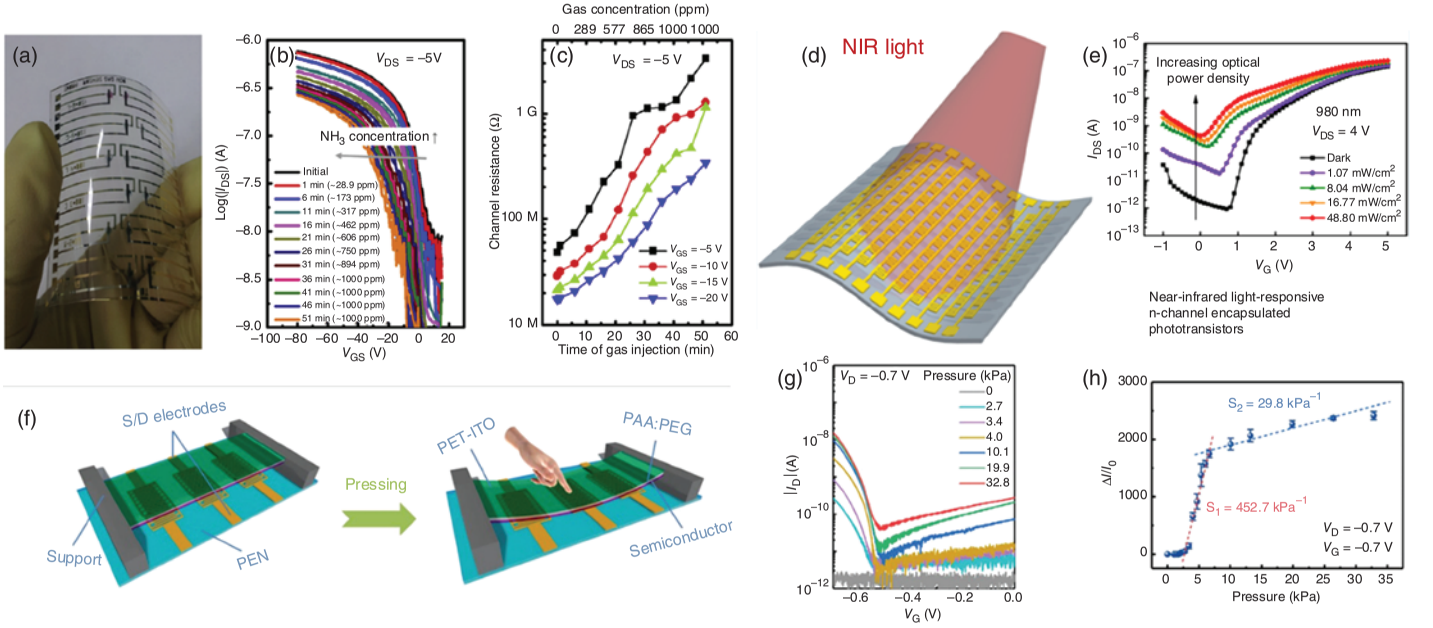

Figure 1.3 Various OTFT-based flexible sensors. (a) Image of P-29-DPP-SVS OFET showing the BG/TC geometry for the gas sensor, (b) transfer curves, and (c) channel resistance of P-29-DPP-SVS OFET. (d) Near-infrared organic phototransistors array. (e) Increased optical power density when exposed to different density of light. (f) Schematic illustration of the OTFT-based pressure sensor (gap: ≈310 μm) in the initial state (left) and pressed state (right). (g) Transfer characteristics of the OTFT sensor under different pressures. (h) Relative change of I_D in response to external pressure for the OTFT sensor at both constant V_D and V_G of −0.7 V. Source: (a–c) Nketia-Yawson et al. 2017 [33]. Reproduced with permission of American Chemical Society; (d, e) Wang et al. 2018 [34]. Reproduced with permission of American Chemical Society; (f–h) Liu et al. 2018 [36]. Reproduced with permission of John Wiley & Sons.

Flexible OTFTs using the PAA:PEG dielectrics showed good universality and greatly enhanced electrical performance under a much smaller operating voltage of –0.7 V than those with a pristine PAA dielectric. The low-voltage OTFTs also exhibited excellent flexibility and bending stability under various bending radii and long cycles. Flexible OTFT-based pressure sensors with low-voltage operation and superhigh sensitivity were demonstrated by using a suspended semiconductor/dielectric/gate structure in combination with the PAA:PEG dielectric, as shown in Figure 1.3g,h. The sensors delivered a record high sensitivity of 452.7 kPa^{-1} under a low voltage of −0.7 V, and excellent operating stability over 5000 cycles. The OTFT sensors were built into a wearable sensor array for spatial pressure mapping, which demonstrates the bright potential of flexible electronics for wearable devices and smart skins.

Apart from polymer and small molecule based transistors, CNTs have also been explored in transistor applications. Han and coworkers demonstrated a large-area high-performance flexible pressure sensor built on an active matrix of 16 × 16 carbon nanotube thin-film transistors (CNT TFTs) [37]. The active matrix exhibited superior flexible thin-film transistor (TFT) performance with high mobility and large current density, along with a high device yield of nearly 99% over a 4-in. sample area. The fully integrated flexible pressure sensor operated within a small voltage range of 3 V and exhibited superb performance featuring a high spatial resolution of 4 mm, faster response than human skin (<30 ms), and excellent accuracy in sensing complex objects on both flat and curved surfaces (Figure 1.4a,b). This work paved the road for future integration of high-performance electronic skin in smart robotics and prosthetic solutions.

Because of its narrow band gap, graphene generally does not exhibit semiconducting behavior. However, in the area of sensing, graphene-based transistors can be successfully fabricated as only the sensing functionality is needed. Also, graphene can be easily functionalized. Lee and coworkers demonstrated a flexible strain sensor based on a reduced graphene oxide field-effect transistor (rGO FET) with ultrasensitivity, stability, and repeatability for the detection of tensile and compressive strains [38]. The novelty of the rGO FET strain sensor is the incorporation of an rGO channel as a sensing layer in which the electrical resistance can be greatly modified upon application of an extremely low level of strain resulting in an intrinsically amplified sensing signal. The rGO FET device was ultrasensitive to extremely low strain levels, as low as 0.02%. Owing to weak coupling between adjacent nanosheets, therefore, upon applying small levels of strain into the rGO thin film, a modulation of the inter-nanosheet resistance is expected, inducing a large change in the transconductance of the rGO FET. Using a simple printing and self-assembly process, the facile fabrication of an rGO FET array over a large area was also demonstrated. In addition, the device was shown to be able to detect small and rapid physical movements of the human body.

A mixture of the organic semiconducting layer or dielectric layers is also a general strategy for improving sensing performance. Moreover, this approach can also impart mechanical stretchability leading to stretchable electronics. Yu and coworkers introduced an all solution-processed type of electronics and sensors that are rubbery and intrinsically stretchable as an outcome

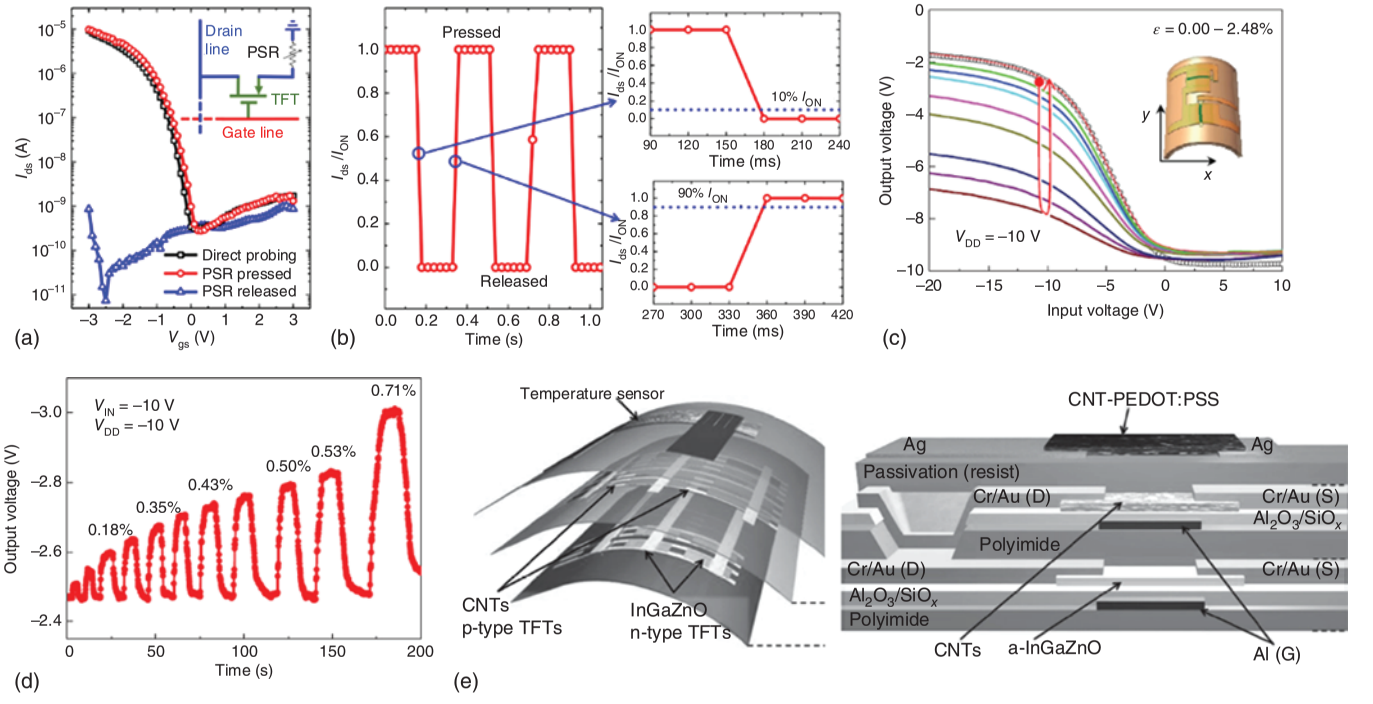

Figure 1.4 (a) $I_{ds} - V_{gs}$ transfer curves at $V_{ds} = -1$ V for an individual pixel when directly probing through the source pad (black), when the PSR is pressed (red), and when the PSR is released (blue), respectively. The inset shows the circuit diagram for a single pixel in the pressure sensor. (b) Time-resolved measurement of the sensor response between pressed and released states. The time resolution of the measurement equipment is 30 ms. The zoomed insets are used to extract the fall time when the weight is lifted (top panel) and the rise time when the weight is dropped (bottom panel). (c) Voltage transfer characteristics of the inverter-type heptazole-based strain gauge, as obtained by a sweeping input voltage from V_{IN} −20 to 10 V: vertical strain bending on driver TFT but horizontal bending on load as shown in the inset, which leads to (d) the output voltage dynamics. (e) Schematic of a vertically integrated 3D flexible CMOS and sensor device. Source: (a, b) Nela et al. 2018 [37]. Reproduced with permission of American Chemical Society; (c, d) Nam et al. 2014 [40]. Reproduced with permission of John Wiley & Sons; (e) Honda et al. 2015 [41]. Reproduced with permission of John Wiley & Sons.

from all the elastomeric materials in percolated composite formats with poly(3-hexylthiophene-2,5-diyl) nanofibrils (P3HT-NFs) and Au nanoparticles with conformally coated silver nanowires (AuNP–AgNW) in PDMS [39]. The fabricated TFTs retained more than 55% of their electrical performances upon 50% stretching and exhibited one of the highest P3HT-based field-effect mobilities of 1.4 $cm^2/(V\,s)$, owing to improved crystallinity. Rubbery sensors, which include strain, pressure, and temperature sensors, exhibit reliable sensing capabilities and can be exploited as smart skins that enable translation of gestures for sign language alphabet and haptic sensing for robotics, illustrating one application of these sensors.

The advantages of transistors also include their ability to be integrated into facial systems for signal amplification. Im and coworkers reported a nonclassical organic strain gauge as a voltage signal sensor using an inverter-type TFT circuit, which sensitively measured a large quantity of elastic strain (up to ≈2.48%) [40]. Heptazole-based organic TFTs were chosen to be incorporated in this gauge circuit, because of the small domain size of the organic solid heptazole. While large crystal domain-pentacene TFTs seldom show sufficient current variation upon mechanical bending for tensile strain, these heptazole TFTs demonstrated a significant variation for the same strain condition as applied to the pentacene alternatives, as shown in Figure 1.4c,d. In addition, the pentacene channel does not recover to its original electric state after bending. In contrast, heptazole channels are very elastic and reversible, even after serious bending. More interesting is the observation that the heptazole TFTs show only minimum variation of signal current under horizontal direction strain, while they make a significant amount of current decrease under vertical direction strain. Utilizing the anisotropic response to the tensile bending strain, an ultrasensitive voltage output strain gauge composed of a horizontally and vertically oriented TFT couple was demonstrated. A complementary inverter using n-type InGaZnO- and p-type CNT-TFTs was also adopted in the area of sensing. Takei and coworkers reported this vertically integrated 3D complementary metal-oxide semiconductor (CMOS) with a temperature sensor device on a flexible substrate; the structure is shown in Figure 1.4e [41]. Relative to conventional lateral integration, this vertical integration process for a flexible device realized high-density integration by adding only ≈4 μm thickness of the flexible passivation layers. The mechanical reliability and temperature dependence of the 3D CMOS inverters were characterized for the first time. These inverters exhibited good mechanical flexibility and relatively stable temperature dependence without a change in performance.

More importantly, vertical integration of both TFTs and sensors facilitated the fabrication of highly integrated and flexible devices for practical low-cost electronics. The introduction of sensor arrays is also a general strategy to improve sensing capability and selectivity. Park and coworkers successfully demonstrated a general approach to fabricate e-skin that can (i) extract effects from the target sensing signals, such as P or T, while the flexible sensor is under multimode stimulus; and (ii) enable real-time bimodal sensing using a single field-effect transistor (FET) device by extracting parameters associated with mechanical deformation [42]. The advantages in integrating FET arrays with

multimodal sensing elements in flexible e-skin greatly reduced the complexity in structural integration, eliminated or minimized the signal interference coupled by strain, significantly reduced the power consumption, and decreased the failure rate in production due to facile integration of FET devices into the circuits. Furthermore, it has potential for reducing fabrication costs of large-area flexible e-skins. This approach may be extended to realize multimodality in large-area flexible e-skin with heterogeneous input stimuli of physical, chemical, or biological nature, and also to solve problems associated with strains induced during operative service of flexible electronic systems.

1.2.3 Electrochemical Sensors

1.2.3.1 Definitions and Important Parameters

Similar to OFETs, electrochemical sensors usually consist of three electrodes, including the reference, the counter, and the working electrodes [43]. Among all the geometries of electrochemical-based sensors, organic electrochemical transistors (OECTs) have received much more attention due to the structure similar to that of conventional transistors, which facilitates fabrication and characterization [44]. Generally, OECTs are comprised of a (semi)conductive polymer, and an electrolyte acting as the dielectric. The gate electrode is immersed in the electrolyte to apply gate bias. Owing to the ultra-large capacitance, OECTs can be effectively driven at voltages lower than 1 V. Moreover, as a kind of transistor, they have all the advantages of transistors. In addition, a fascinating feature of OECTs is that the electrolyte acts as a dielectric and can be used as a sensing medium. Owing to the double layer capacitor characteristics, the geometry of an OECT can be easily adjusted [45]. In the following section, we will focus more on OECT-based sensors.

1.2.3.2 Strategy and Applications

Owing to their unique device properties, OECTs are more attractive when applied in the area of stretchable and wearable sensors, as their dielectrics are either liquid or ultra-stretchable gel materials. Furthermore, OECTs are extremely compatible with biosensor applications, as their behavior is very similar to that of the synapse. Lee et al. reported an organic optoelectronic sensorimotor synapse that uses an organic optoelectronic synapse and a neuromuscular system based on a stretchable organic nanowire synaptic transistor (s-ONWST) [46]. The voltage pulses of a self-powered photodetector triggered by optical signals drive the s-ONWST, and the resultant informative synaptic outputs were used not only for optical wireless communication of human–machine interfaces but also for light-interactive actuation of an artificial muscle actuator in the same way that a biological muscle fiber contracts. This organic optoelectronic sensorimotor synapse suggests a promising strategy toward developing bioinspired soft electronics, neurologically inspired robotics, and electronic prostheses.

Other than organic small molecules and polymers, CNTs were also applied in electrochemical sensors. Huang and coworkers reported an attractive stretchable electrochemical sensor that takes advantage of a hierarchical percolation

network of carbon nanotubes and gold nanotubes (CNTsAu NTs) [47]. This hybrid nanostructure provided the sensor with excellent time-reproducible mechanical and electrochemical performance while granting very good cellular compatibility, making it perfectly apt to induce and monitor simultaneously transient biochemical signals. This is validated by monitoring the stretch-induced transient release of small signaling molecules by both endothelial and epithelial cells cultured on this sensor and submitted to stretching strains of different intensities, as shown in Figure 1.5a–d. This work demonstrates that the hybrid CNTs-Au NTs platform offers a versatile and highly sensitive approach to characterize and quantify short-time mechano-transduction responses.

Natural organic materials have also been widely utilized as active sensing materials of electrochemical-based sensors. Wang and coworkers developed a flexible glove-based electrochemical biosensor with a highly stretchable printed electrode system as a wearable point-of-use screening tool for defense and food security applications by adopting an enzyme [48]. This disposable, mechanically robust "lab-on-a-glove" integrated a stretchable printable enzyme-based biosensing system and active surface for swipe sampling on different fingers and was coupled with a compact electronic interface for electrochemical detection and real-time wireless data transmission to a smartphone device (Figure 1.5e–j). Stress enduring inks were used to print the electrode system and the long serpentine connections to the wireless electronic interface. Dynamic mechanical deformation, bending, and stretching studies illustrated the resilience and compliance of the printed traces against extreme mechanical deformations

Figure 1.5 (a) Fluorescence microscopic image of mechanically strained HUVECs (30% stretch) after staining with Alexa Fluor 488 phalloidin (green: actin fibers) and Hoechst 33342 (blue: nuclei). (b) Schematic diagram of cellular mechanotransduction mechanism stimulated in stretched cells. (c) Current responses detected from HUVECs submitted to different stretch moduli (I–III) (see text). (d) Current responses detected from HBECs submitted to different stretch moduli. The vertical gray dashed lines in (c) and (d) indicate the beginning points of mechanical stretches; it took five seconds to achieve the desired strains. The electrode was submitted to a cycle of stretch and release process before applying another stretch episode to the cells. (e) Image of the serpentine stencil design employed for printing the glove-based stretchable device. (f) Schematic of (left) the biosensing scan finger (index finger) containing smiling face shaped carbon-based counter (CE), working (WE) electrodes and Ag/AgCl-based reference electrode (RE), and (right) collecting thumb finger with its printed carbon pad; scale bar 10 mm. (g) Photographs of the biosensing index finger under 0% (left) and 50% (right) linear stretch; scale bar, 10 mm. (h) On-glove swiping protocol for sampling chemical threat residues from tomato and stainless steel surfaces. (i) On-glove sensing procedure by joining the index (scan) and thumb (collector) fingers to complete the electrochemical cell. (j) Photographs of the wearable glove biosensor, consisting of a sensing finger, containing the immobilized OPH enzyme layer, and the collector/sampling finger. (k) Schematic illustration of the current change mechanism for detecting target PSA molecules attached to the sensor surface. (l, m) Kinetic monitoring of PSA binding to rGO@SFP-based biosensor without and with immobilized anti-PSA antibodies. (n) The response time of rGO@SFP-based biosensor detection against 1×10^{-12} M target PSA. Source: (a–d) Liu et al. 2017 [47]. Reproduced with permission of John Wiley & Sons; (e–j) Mishra et al. 2017 [48]. Reproduced with permission of Royal Society of Chemistry; (k–n) Wang et al. 2016 [49]. Reproduced with permission of John Wiley & Sons.

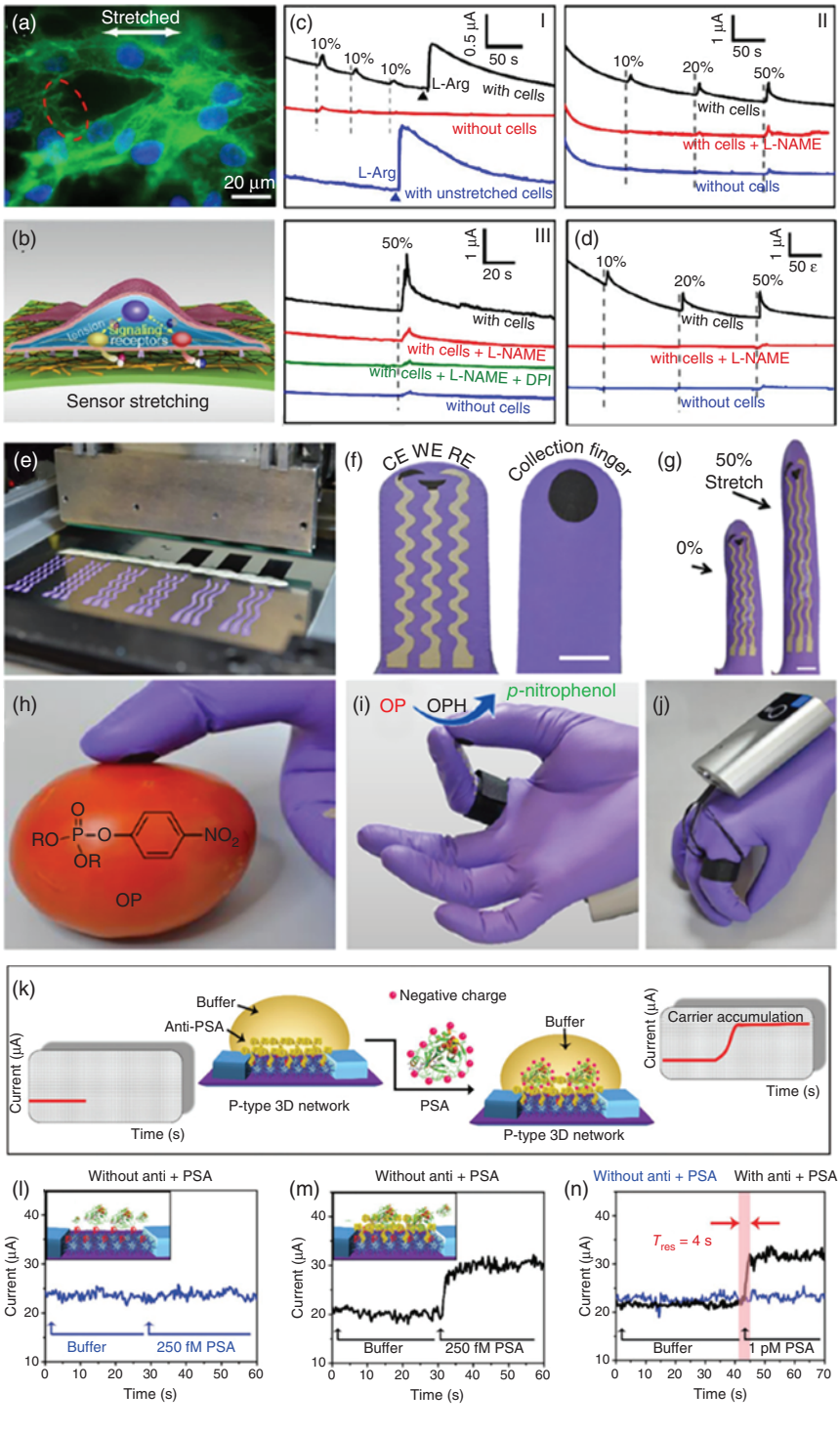
(a)
Stretched
20 μm
(b)
Tension
Signaling receptors
Sensor stretching
(c)
I
0.5 μA
50 s
10%
10%
10%
L-Arg
with cells
without cells
L-Arg
with unstretched cells
II
1 μA
50 s
10%
20%
50%
with cells
with cells + L-NAME
without cells
III
50%
1 μA
20 s
with cells
with cells + L-NAME
with cells + L-NAME + DPI
without cells
(d)
1 μA
50 ε
10%
20%
50%
with cells
with cells + L-NAME
without cells
(e)
(f)
CE WE RE
Collection finger
(g)
50%
Stretch
0%
(h)
RO
O
P
O
OR
NO2
OP
(i)
OP
OPH
p-nitrophenol
(j)
(k)
Buffer
Anti-PSA
P-type 3D network
Negative charge
PSA
Buffer
P-type 3D network
Current (μA)
Time (s)
Carrier accumulation
Current (μA)
Time (s)
(l)
Without anti + PSA
Current (μA)
Buffer
250 fM PSA
Time (s)
(m)
Without anti + PSA
Current (μA)
Buffer
250 fM PSA
Time (s)
(n)
Without anti + PSA
With anti + PSA
Tres = 4 s
Current (μA)
Buffer
1 pM PSA
Time (s)

expected for such on-glove sampling/sensing operation. An organophosphorus hydrolase (OPH)-based biosensor system on the index finger enabled rapid on-site detection of organophosphate (OP) nerve agent compounds on suspicious surfaces and agricultural products following their swipe collection on the thumb finger. The new wireless glove-based biosensor system offers considerable promise for field screening of OP nerve agents and pesticides in defense and food safety applications, with significant speed and cost advantages. Such "lab-on-a-glove" demonstration opened the area of flexible wearable sensors to future on-the-hand multiplexed chemical detection in diverse fields. Other than pure natural organic materials for active layer, they were also coupled with graphene to enhance sensing performance. Cho and coworkers described an ultrasensitive, flexible sensor as a 3D hierarchical biocomposite comprising of hollow, natural pollen microcapsules that were coated with a conductive graphene layer [49]. Modular assembly of the graphene-coated microcapsules onto an ultrathin polyethylene terephthalate layer enables a highly flexible sensor configuration with tunable selectivity afforded by subsequent covalent immobilization of antibodies against target antigens. In a proof-of-concept example, the biosensor demonstrated ultrahigh sensitivity detection of prostate-specific antigen (PSA) down to 1.7×10^{-15} m with real-time feedback and superior performance over conventional two-dimensional graphene-coated sensors (Figure 1.5k–n). Importantly, the device performance was consistently high across various bending conditions. Taken together, the results demonstrated in this work highlight the merits of employing lightweight biocomposites as modular building blocks for the design of flexible biosensors with highly responsive and sensitive molecular detection capabilities.

1.2.4 Diode-Based Sensors

1.2.4.1 Definitions and Important Parameters

A diode is a two-terminal device that contains a p-type and an n-type material to form a p–n junction and has the property of only conducting current in one direction. In the sensing area, diodes have been widely used in the form of photodetectors, in which the current of the diode is extremely sensitive to the light illumination [50]. Key parameters include photosensitivity, response/recovery time. A single photodetector can be utilized to realize environmental light sensing. By coupling with a light-emitting diode, it can be used to detect human health information such as heart rate, blood pressure, and oxygen and glucose levels in the blood. This kind of device has already been commercialized for decades. In recent years, with the emergence of organic materials, further development with flexible, even wearable photosensors has occurred, targeting next-generation portable health monitoring.

1.2.4.2 Strategy and Applications

For the acquisition of health information, organic materials-based light-emitting diodes have been designed for emission of purer light, leading to improved accuracy of the photodetectors. Arias and coworkers presented a method to print two materials of different functionality during the same printing step [51]. In printed

electronics, devices are built layer by layer and conventionally only one type of material is deposited in one pass. Here, the challenges involving the printing of two emissive materials to form polymer light-emitting diodes (PLEDs) that emit light of different wavelengths without any significant changes in the device characteristics were described. The surface-energy-patterning technique was utilized to print materials in regions of interest. This technique proved beneficial in reducing the amount of ink used during blade coating and improving the reproducibility of printed films. A variety of colors (green, red, and near-infrared) were demonstrated and characterized. This is the first known attempt to print multiple materials by blade coating. These devices were further used in conjunction with a commercially available photodiode to perform blood oxygenation measurements on the wrist, where common accessories are worn. Prior to the actual application, the threshold conditions for each color were determined in order to acquire a stable and reproducible photoplethysmogram (PPG) signal. Finally, based on the conditions, PPG and oxygenation measurements were successfully performed on the wrist with green and red PLEDs. Yoo and coworkers exploited the design freedom offered by organic technologies to realize a reflective patch-type pulse oximetry sensor with ultralow power consumption [52]. On the basis of flexible OLEDs and organic photodiodes designed via an optical simulation of color-sensitive light propagation within the human skin, the proposed monolithically integrated organic pulse oximetry sensor heads exhibit successful operation at electrical power as low as 24 mW on average.

1.2.5 Other Devices and System Integration

Other than the abovementioned four types of devices, other devices can also be fabricated to function as sensors [53]. Dickey and coworkers described the fabrication and characterization of soft and stretchable capacitive sensors of torsion, strain, and touch using hollow elastomeric fibers [54]. Twisting or elongating an intertwined bundle of two fibers increased the contact area between the fibers and therefore the capacitance. Additionally, bundles of fibers filled with LM can serve as capacitive touch sensors along the length of the bundle by using fibers filled with metal to various lengths. These sensors were able to detect touch via self-capacitance with the finger, rather than by physical deformation. Because these fiber sensors are extremely soft and stretchable, as well as small ($\approx$200–800 μm diameter), they could be used with artificial muscles, soft robotics, and stretchable devices. They have higher detection limits than state-of-the-art sensors; however, they can measure large ranges of torsion and strain and have an advantageous fiber shape that can conform to a variety of complex surfaces. As the modes for sensing torsion, strain, and touch all rely on capacitance, it is currently not possible to decouple them, although future work could measure other electrical properties, such as resistance, to help decouple their effects. For these fibers to be utilized in fabrics, further work must be done to understand their cyclic behavior and wash resistance; however, these fibers offer a promising opportunity to create woven and wearable sensors in stretchable textiles for a variety of sensing functions.

To reveal the potential of various devices and materials, a systems integration strategy has been extensively utilized [55]. With systems integration, ultrahigh selectivity and in-situ multiparameter monitoring can be realized, even though these are not accessible within a single device [56]. System integration is applied in force sensors at the very beginning. Kyung and coworkers developed a fast responding force sensor array that detects multiple points; it is thin, highly transparent, and highly flexible; and it is based on polymer waveguides that can be applied to curvilinear interfaces [57]. The force sensor detects contact forces by monitoring light intensity transmitted through sensing areas that allow a touch layer to be in contact with the bare core of the waveguide patterns. The force sensor is capable of working without any electronic components on the sensing areas. The response characteristics including sensitivity, response time, and hysteresis depend on the mechanical properties of the touch layers. The use of the touch layer allowed the force sensor to provide a fast and sensitive response without significant hysteresis to the programmed sinusoidal input force (c. 0–3 N) with frequency in the range of 1–16 Hz. The response was also highly durable over 3600 continuous loading and unloading cycles and resistant to bending. The thin-film architecture with the combination of the waveguide sensing mechanism and soft optical materials allowed the demonstration of detection of simultaneous and multiple forces on a curvilinear surface such as the human arm. When the sensor is practically applied to electronic devices as a flexible input interface, it may additionally be applicable to the analysis of environmental effects such as temperature and humidity.

We also need to investigate the optimal spatial pattern for power consumption and materials for rapid response with low hysteresis. Wang and coworkers reported a self-powered triboelectric sensor based on flexible thin-film materials. It relies on contact electrification to generate a voltage signal in response to a physical contact without using an external power supply [58]. Enabled by the sensing mechanism and surface modification by polymer nanowires, the triboelectric sensor exhibited an exceptional pressure sensitivity of 44 mV/Pa (0.09% Pa^{-1}) and a maximum touch sensitivity of 1.1 V/Pa (2.3% Pa^{-1}) in the extremely low-pressure region (<0.15 kPa). Through the integration of the sensor with a signal-processing circuit, a complete tactile sensing system was further developed. Diverse applications were demonstrated, explicitly indicating a variety of immediate uses in the human–electronics interface, automatic control, surveillance, remote operation, and security systems, as shown in Figure 1.6a–f.

Chan and coworkers had demonstrated a temperature-sensor device based on a large-area flexible OFET array [59]. By utilizing an ultrathin PEN substrate, the device can be conformally attached to various objects or the human body. The electrochemically grown alumina was adopted as the dielectric, which allowed the device to operate below 4 V and maintain a leakage current approximately in the range of tens of pA. The fabrication technique is not limited to temperature sensors, but can also be utilized as a driving/switching circuit for other devices in array form, such as light-emitting diode (LED) back panels. By controlling the nominal thickness of the Ag NPs, both the conductivity and sensitivity of thermistors can be tuned. The integrated temperature sensor maintained more than

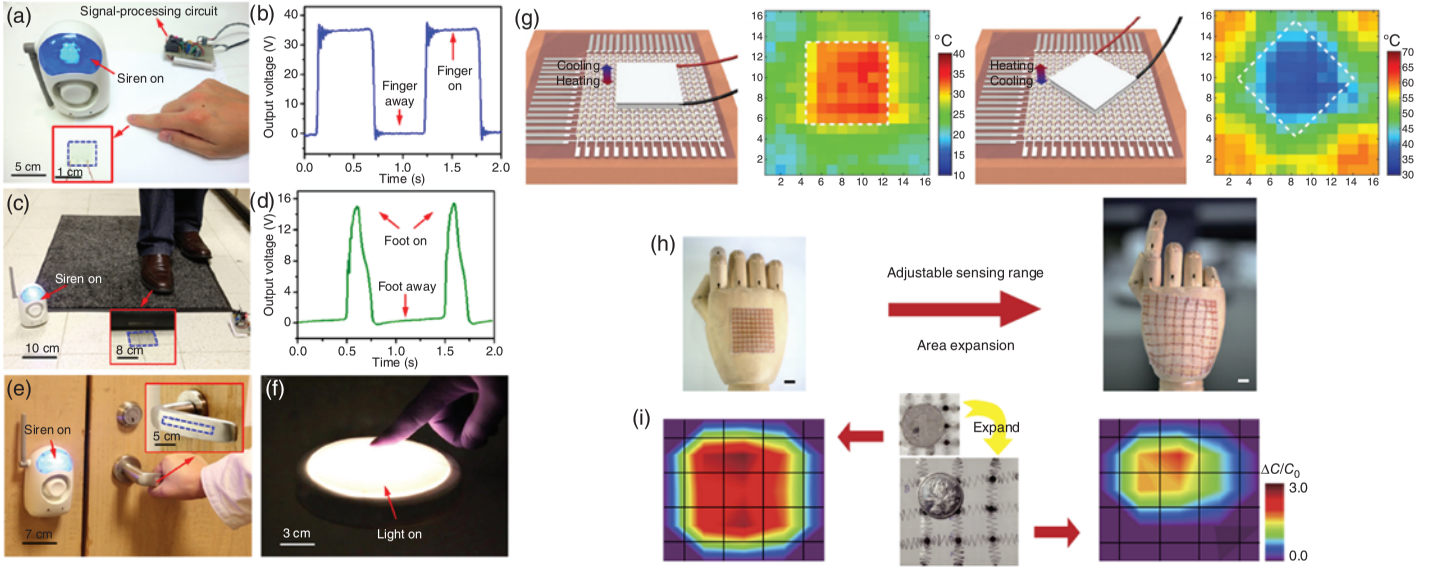

Figure 1.6 (a) Triggering a wireless alarm system by gentle finger tapping on a TES (1 cm in side length). Inset: enlarged view of the TES on a piece of paper. (b) Output voltage of the TES generated by finger tapping. (c) Triggering a wireless alarm system by stepping on top of a TES (10 cm in side length) that is embedded underneath a carpet. Inset: enlarged view of the TES on the floor. (d) Output voltage generated by stepping on the TES covered by the carpet. (e) Triggering a wireless alarm system by grabbing the TES (5 cm by 3 mm) that is applied on a door handle. Inset: enlarged view of the TES on the door handle. (f) Switching a panel light by finger tapping on the TES (1 cm in side length) that is applied on the surface of the light. (g) Schematic diagram of temperature measurement setup; a Peltier heater is placed on top of the sensor array, and the base of the Peltier heater warms up/cools down the region of the sensor array, with temperature distribution measured from the sensor array; the dashed lines indicate where the Peltier heater is located. (h) Schematic illustration of an SCMN as an artificial electronic skin on a hand, showing sensing adjustability and expandability (scale bar: 1 cm). (i) Pressure mapping before and after the 300% expansion of an SCMN; the position of the pressure load is also identified after expansion. Source: (a–f) Zhu et al. 2014 [58]. Reproduced with permission of American Chemical Society; (g) Xia et al. 2016 [59]. Reproduced with permission of Royal Society of Chemistry; (h, i) Ye et al. 2018 [60]. Reproduced with permission of Springer Nature.

20 times the output current change, while the operating temperature changed from 20 to 100 °C. The actively addressed 16 × 16 OFET array attained a 100% yield rate and provided 2D temperature information of the contacted objects, including those with irregular shapes. As shown in Figure 1.6g, the current device enabled defect prediction of electronic devices, remote sensing of harsh environments, food supply chain management, and e-skin applications. Attaching the temperature-sensor array onto the outside of the human body or its organs during surgery may provide valuable thermal distribution information that could be useful for diagnostic and therapeutic purposes.

A multifunctional sensor array has also been realized with systems integration. Wang and coworkers presented a skin-inspired highly stretchable and conformable matrix network (SCMN) that successfully expanded the e-skin sensing functionality including but not limited to temperature, in-plane strain, humidity, light, magnetic field, pressure, and proximity [60]. The actualized specific expandable sensor units integrated on a structured polyimide network, potentially in a three-dimensional (3D) integration scheme, can also fulfill simultaneous multi-stimulus sensing and achieve an adjustable sensing range and large-area expandability (Figure 1.6h,i). A personalized intelligent prosthesis was further constructed and demonstrated its use in real-time spatial pressure mapping and temperature estimation. Looking forward, this SCMN has broader applications in humanoid robotics, new prosthetics, human–machine interfaces, and health-monitoring technologies. Takei and coworkers presented a flexible, multifunctional printed health-care sensor equipped with a three-axis acceleration sensor to monitor physical movement and motion [61]. Because the device was designed to be attached directly onto the skin, it had a modular design with two detachable components: one device component was nondisposable, whereas the other one was disposable and designed to be worn in contact with the skin. The design of this disposable sensing sheet takes into account hygiene concerns and low-cost materials and fabrication methods as well as features including integrated, printed sensors to monitor for temperature, acceleration, electrocardiograms, and a kirigami structure, which allows for stretching on the skin. The reusable component contains more expensive device components, featuring an ultraviolet light sensor that is controlled by CNT TFTs and has a mechanically flexible and stable liquid metal contact for connection to the disposable sensing sheet. After characterizing the electrical properties of the transistors and flexible sensors, a proof-of-concept device was demonstrated that is capable of health-care monitoring combined with detection of physical activity, showing that this device provides an excellent platform for the development of commercially viable, wearable health-care monitors.

1.3 Summary and Perspective

The development of organic nano-sensors is well on its way to realizing commercialization. Owing to the flexible, stretchable properties of organic functional materials, they are among the most promising materials that can be used in wearable sensors. Currently, there is tremendous demand for better monitoring of

human health and recording of environmental parameters. As the most important interconnection part of this process, sensors play a key role in timely, accurate information collection. Accompanied with other wearable active constituent parts, including a wearable power source, stretchable electrical interconnection, and lightweight information processor, the practical commercialization of smart clothing can be expected in the near future.

Until now, several major challenges continue to impede the further development of wearable sensors [62]. Stability is one of the most stubborn problems for organic materials. Stability specifically refers to the long-lived activities under working conditions, e.g. the bias stability of transistors under light exposure or analyte chemical exposure. Another important stability parameter relates to whether the sensor performance is robust when functioning under situations of bending, twisting, or stretching. A well-recognized standard to quantify the stability properties is still missing, but it is believed that such standard will soon be established, along with the massive production of smart clothing. Biocompatibility is another important issue for organic materials-based sensors. For accurate measurement of human health information, most of the organic nano-sensors are directly applied to human skin, and even implanted into tissues and organs. Thus, the toxicity of organic materials must be carefully examined, and any massive commercialization and experimental trials should take safety as the first priority. Multidisciplinary collaboration will serve as the most effective strategy to promote the further development of wearable organic nano-sensors, with the participation of organic chemists for new materials development, the materials, mechanical and electrical engineers for materials evaluation, optimization, and device fabrication, as well as the clinicians for applications in human health monitoring.

References

1 Han, S.T., Peng, H., Sun, Q. et al. (2017). *Adv. Mater.* 29: 1700375.

2 (a) Zhao, S., Li, J., Cao, D. et al. (2017). *ACS Appl. Mater. Interfaces* 9: 12147. (b) Zang, Y.P., Zhang, F.J., Di, C.A., and Zhu, D.B. (2015). *Mater. Horiz.* 2: 140.

3 (a) Xu, M., Obodo, D., and Yadavalli, V.K. (2019). *Biosens. Bioelectron.* 124–125: 96. (b) Xie, M., Hisano, K., Zhu, M. et al. (2019). *Adv. Mater. Technol.* 4: 1800626.

4 Kim, S.J., Choi, S.J., Jang, J.S. et al. (2017). *Acc. Chem. Res.* 50: 1587.

5 (a) Wang, X., Liu, Z., and Zhang, T. (2017). *Small* 13: 1602790. (b) Ramasamy, M., Kumar, P.S., and Varadan, V.K. (2017). *Nanosens Biosens Info Tech Sens 3D Syst* 10167: 1016703.

6 (a) Matzeu, G., Florea, L., and Diamond, D. (2015). *Sens. Actuators, B* 211: 403. (b) Lou, Z., Wang, L., and Shen, G. (2018). *Adv. Mater. Technol.* 3: 1800444.

7 (a) Lee, Y.H., Kweon, O.Y., Kim, H. et al. (2018). *J. Mater. Chem. C* 6: 8569. (b) Kim, J., Jeerapan, I., Sempionatto, J.R. et al. (2018). *Acc. Chem. Res.* 51: 2820.

8 Kleinschmidt, A.T. and Lipomi, D.J. (2018). *Acc. Chem. Res.* 51: 3134.
9 Andrew, T.L., Zhang, L., Cheng, N. et al. (2018). *Acc. Chem. Res.* 51: 850.
10 (a) Tian, L., Li, Y., Webb, R.C. et al. (2017). *Adv. Funct. Mater.* 27: 1701282. (b) Tessarolo, M., Gualandi, I., and Fraboni, B. (2018). *Adv. Mater. Technol.* 3: 1700310.
11 Neethirajan, S. (2017). *Sens. Biosens. Res.* 12: 15.
12 Nag, A., Mukhopadhyay, S.C., and Kosel, J. (2017). *IEEE Sens. J.* 17: 3949.
13 Rim, Y.S., Bae, S.H., Chen, H. et al. (2016). *Adv. Mater.* 28: 4415.
14 Hou, C., Wang, H., Zhang, Q. et al. (2014). *Adv. Mater.* 26: 5018.
15 Wang, Y., Wang, L., Yang, T.T. et al. (2014). *Adv. Funct. Mater.* 24: 4666.
16 Duy, L.T., Trung, T.Q., Dang, V.Q. et al. (2016). *Adv. Funct. Mater.* 26: 4329.
17 Lipomi, D.J., Vosgueritchian, M., Tee, B.C. et al. (2011). *Nat. Nanotechnol.* 6: 788.
18 Karimov, K.S., Saleem, M., Karieva, Z.M. et al. (2011). *Phys. Scr.* 83: 065703.
19 Li, L., Bai, Y., Li, L. et al. (2017). *Adv. Mater.* 29: 1702517.
20 Darabi, M.A., Khosrozadeh, A., Mbeleck, R. et al. (2017). *Adv. Mater.* 29: 1700533.
21 Huynh, T.P. and Haick, H. (2016). *Adv. Mater.* 28: 138.
22 Wang, Q., Jian, M., Wang, C., and Zhang, Y. (2017). *Adv. Funct. Mater.* 27: 1605657.
23 Liu, H., Li, M., Ouyang, C. et al. (2018). *Small* 14: e1801711.
24 Pang, Y., Tian, H., Tao, L. et al. (2016). *ACS Appl. Mater. Interfaces* 8: 26458.
25 Zhou, X., Zhu, L., Fan, L. et al. (2018). *ACS Appl. Mater. Interfaces* 10: 31655.
26 Cai, Y., Shen, J., Dai, Z. et al. (2017). *Adv. Mater.* 29: 1606411.
27 Chellattoan, R., Lube, V., and Lubineau, G. (2018). *Adv. Electron. Mater.* 5: 1800273.
28 Yu, X.G., Zhou, N.J., Han, S.J. et al. (2013). *J. Mater. Chem. C* 1: 6532.
29 Zang, Y., Huang, D., Di, C.A., and Zhu, D. (2016). *Adv. Mater.* 28: 4549.
30 Lee, Y.H., Jang, M., Lee, M.Y. et al. (2017). *Chem* 3: 724.
31 Lee, M.Y., Lee, H.R., Park, C.H. et al. (2018). *Acc. Chem. Res.* 51: 2829.
32 Ryu, G.S., Park, K.H., Park, W.T. et al. (2015). *Org. Electron.* 23: 76.
33 Nketia-Yawson, B., Jung, A.R., Noh, Y. et al. (2017). *ACS Appl. Mater. Interfaces* 9: 7322.
34 Wang, G., Huang, K., Liu, Z. et al. (2018). *ACS Appl. Mater. Interfaces* 10: 36177.
35 Wu, X.H., Ma, Y., Zhang, G.Q. et al. (2015). *Adv. Funct. Mater.* 25: 2138.
36 Liu, Z., Yin, Z., Wang, J., and Zheng, Q. (2018). *Adv. Funct. Mater.*: 1806092.
37 Nela, L., Tang, J., Cao, Q. et al. (2018). *Nano Lett.* 18: 2054.
38 Trung, T.Q., Tien, N.T., Kim, D. et al. (2014). *Adv. Funct. Mater.* 24: 117.
39 Kim, H.J., Sim, K., Thukral, A., and Yu, C. (2017). *Sci. Adv.* 3: e1701114.
40 Nam, S.H., Jeon, P.J., Min, S.W. et al. (2014). *Adv. Funct. Mater.* 24: 4413.
41 Honda, W., Harada, S., Ishida, S. et al. (2015). *Adv. Mater.* 27: 4674.
42 Tien, N.T., Jeon, S., Kim, D.I. et al. (2014). *Adv. Mater.* 26: 796.
43 Yang, M., Jeong, S.W., Chang, S.J. et al. (2016). *ACS Appl. Mater. Interfaces* 8: 34978.
44 Yang, A., Li, Y., Yang, C. et al. (2018). *Adv. Mater.* 30: e1800051.
45 Shiwaku, R., Matsui, H., Nagamine, K. et al. (2018). *Sci. Rep.* 8: 6368.

46 Lee, Y., Oh, J.Y., Xu, W. et al. (2018). *Sci. Adv.* 4: eaat7387.
47 Liu, Y.L., Qin, Y., Jin, Z.H. et al. (2017). *Angew. Chem. Int. Ed. Engl.* 56: 9454.
48 Mishra, R.K., Hubble, L.J., Martín, A. et al. (2017). *ACS Sens.* 2: 553.
49 Wang, L.L., Jackman, J.A., Ng, W.B., and Cho, N.J. (2016). *Adv. Funct. Mater.* 26: 8623.
50 Wu, Z., Zhai, Y., Kim, H. et al. (2018). *Acc. Chem. Res.* 51: 3144.
51 Han, D., Khan, Y., Ting, J. et al. (2017). *Adv. Mater.* 29: 1606206.
52 Lee, H., Kim, E., Lee, Y. et al. (2018). *Sci. Adv.* 4: eaas9530.
53 Nakata, S., Shiomi, M., Fujita, Y. et al. (2018). *Nat. Electron.* 1: 596.
54 Cooper, C.B., Arutselvan, K., Liu, Y. et al. (2017). *Adv. Funct. Mater.* 27: 1605630.
55 (a) Xu, S., Zhang, Y., Jia, L. et al. (2014). *Science* 344: 70. (b) Yang, Y., Zhang, H.L., Lin, Z.H. et al. (2013). *ACS Nano* 7: 9213.
56 Sarwar, M.S., Dobashi, Y., Preston, C. et al. (2017). *Sci. Adv.* 3: e1602200.
57 Yun, S., Park, S., Park, B. et al. (2014). *Adv. Mater.* 26: 4474.
58 Zhu, G., Yang, W.Q., Zhang, T. et al. (2014). *Nano Lett.* 14: 3208.
59 Ren, X., Pei, K., Peng, B. et al. (2016). A low-operating-power and flexible active-matrix organic-transistor temperature-sensor array. *Adv. Mat.* 28 (24): 4832–4838.
60 Ye, L., Hu, H., Ghasemi, M. et al. (2018). *Nat. Mater.* 17: 253.
61 Yamamoto, Y., Harada, S., Yamamoto, D. et al. (2016). *Sci. Adv.* 2: e1601473.
62 Bandodkar, A.J., Jeerapan, I., and Wang, J. (2016). *ACS Sens.* 1: 464.